Unusually High Thermal Conductivity of Carbon Nanotubes

Savas Berber, Young-Kyun Kwon,* and David Tománek

Department of Physics and Astronomy, and Center for Fundamental Materials Research, Michigan State University, East Lansing, Michigan 48824-1116

(Received 23 February 2000)

Combining equilibrium and nonequilibrium molecular dynamics simulations with accurate carbon potentials, we determine the thermal conductivity λ of carbon nanotubes and its dependence on temperature. Our results suggest an unusually high value, $\lambda \approx 6600$ W/m K, for an isolated (10, 10) nanotube at room temperature, comparable to the thermal conductivity of a hypothetical isolated graphene monolayer or diamond. Our results suggest that these high values of λ are associated with the large phonon mean free paths in these systems; substantially lower values are predicted and observed for the basal plane of bulk graphite.

PACS numbers: 61.48.+c, 63.22.+m, 66.70.+f, 68.70.+w

With the continually decreasing size of electronic and micromechanical devices, there is an increasing interest in materials that conduct heat efficiently, thus preventing structural damage. The stiff sp^3 bonds, resulting in a high speed of sound, make monocrystalline diamond one of the best thermal conductors [1]. An unusually high thermal conductance should also be expected in carbon nanotubes [2,3], which are held together by even stronger sp^2 bonds. These systems, consisting of seamless and atomically perfect graphitic cylinders a few nanometers in diameter, are self-supporting. The rigidity of these systems, combined with virtual absence of atomic defects or coupling to soft phonon modes of the embedding medium, should make isolated nanotubes very good candidates for efficient thermal conductors. This conjecture has been confirmed by experimental data that are consistent with a very high thermal conductivity for nanotubes [4].

In the following, we will present results of molecular dynamics simulations using the Tersoff potential [5], augmented by van der Waals interactions in graphite, for the temperature dependence of the thermal conductivity of nanotubes and other carbon allotropes. We will show that isolated nanotubes are at least as good of heat conductors as high-purity diamond. Our comparison with graphitic carbon shows that interlayer coupling reduces thermal conductivity of graphite within the basal plane by 1 order of magnitude with respect to the nanotube value which lies close to that for a hypothetical isolated graphene monolayer.

The thermal conductivity λ of a solid along a particular direction, taken here as the z axis, is related to the heat flowing down a long rod with a temperature gradient dT/dz by

$$\frac{1}{A}\frac{dQ}{dt} = -\lambda \frac{dT}{dz}, \tag{1}$$

where dQ is the energy transmitted across the area A in the time interval dt. In solids where the phonon contribution to the heat conductance dominates, λ is proportional to Cvl, the product of the heat capacity per unit volume C, the speed of sound v, and the phonon mean free path l. The latter quantity is limited by scattering from sample boundaries (related to grain sizes), point defects, and by umklapp processes. In the experiment, the strong dependence of the thermal conductivity λ on l translates into an unusual sensitivity to isotopic and other atomic defects. This is best illustrated by the reported thermal conductivity values in the basal plane of graphite [6] which scatter by nearly 2 orders of magnitude. As similar uncertainties may be associated with thermal conductivity measurements in "mats" of nanotubes [4], we decided to determine this quantity using molecular dynamics simulations.

The first approach used to calculate λ was based on a direct molecular dynamics simulation. Heat exchange with a periodic array of hot and cold regions along the nanotube has been achieved by velocity rescaling, following a method that had been successfully applied to the thermal conductivity of glasses [7]. Unlike glasses, however, nanotubes exhibit an unusually high degree of long-range order over hundreds of nanometers. The perturbations imposed by the heat transfer reduce the effective phonon mean free path to below the unit cell size. We found it hard to achieve convergence, since the phonon mean free path in nanotubes is significantly larger than unit cell sizes tractable in molecular dynamics simulations.

As an alternate approach to determine the thermal conductivity, we used equilibrium molecular dynamics simulations [8,9] based on the Green-Kubo expression that relates this quantity to the integral over time t of the heat flux autocorrelation function by [10]

$$\lambda = \frac{1}{3Vk_BT^2}\int_0^\infty \langle \mathbf{J}(t)\cdot\mathbf{J}(0)\rangle\, dt\,. \tag{2}$$

Here, k_B is the Boltzmann constant, V is the volume, T the temperature of the sample, and the angular brackets denote an ensemble average. The heat flux vector $\mathbf{J}(t)$ is

defined by

$$\mathbf{J}(t) = \frac{d}{dt}\sum_i \mathbf{r}_i \Delta e_i$$

$$= \sum_i \mathbf{v}_i \Delta e_i - \sum_i \sum_{j(\neq i)} \mathbf{r}_{ij}(\mathbf{f}_{ij} \cdot \mathbf{v}_i), \qquad (3)$$

where $\Delta e_i = e_i - \langle e \rangle$ is the excess energy of atom i with respect to the average energy per atom $\langle e \rangle$. $\mathbf{r}_i$ is the position and $\mathbf{v}_i$ the velocity of atom i, and $\mathbf{r}_{ij} = \mathbf{r}_j - \mathbf{r}_i$. Assuming that the total potential energy $U = \sum_i u_i$ can be expressed as a sum of binding energies u_i of individual atoms, then $\mathbf{f}_{ij} = -\nabla_i u_j$, where ∇_i is the gradient with respect to the position of atom i.

In low-dimensional systems, such as nanotubes or graphene monolayers, we infer the volume from the way these systems pack in space (nanotubes form bundles and graphite a layered structure, both with an interwall separation of $\approx$3.4 Å) in order to convert thermal conductance of a system to thermal conductivity of a material.

Once $\mathbf{J}(t)$ is known, the thermal conductivity can be calculated using Eq. (2). We found, however, that these results depend sensitively on the initial conditions of each simulation, thus necessitating a large ensemble of simulations. This high computational demand was further increased by the slow convergence of the autocorrelation function, requiring long integration time periods.

These disadvantages have been shown to be strongly reduced in an alternate approach [11] that combines the Green-Kubo formula with nonequilibrium thermodynamics [12,13] in a computationally efficient manner [14]. In this approach, the thermal conductivity along the z axis is given by

$$\lambda = \lim_{\mathbf{F}_e \to 0} \lim_{t \to \infty} \frac{\langle J_z(\mathbf{F}_e, t) \rangle}{F_e T V}, \qquad (4)$$

where T is the temperature of the sample, regulated by a Nosé-Hoover thermostat [15], and V is the volume of the sample. $J_z(\mathbf{F}_e, t)$ is the z component of the heat flux vector for a particular time t. $\mathbf{F}_e$ is a small fictitious "thermal force" (with a dimension of inverse length) that is applied to individual atoms. This fictitious force $\mathbf{F}_e$ and the Nosé-Hoover thermostat impose an additional force $\Delta\mathbf{F}_i$ on each atom i. This additional force modifies the gradient of the potential energy and is given by

$$\Delta\mathbf{F}_i = \Delta e_i \mathbf{F}_e - \sum_{j(\neq i)} \mathbf{f}_{ij}(\mathbf{r}_{ij} \cdot \mathbf{F}_e)$$

$$+ \frac{1}{N}\sum_j \sum_{k(\neq j)} \mathbf{f}_{jk}(\mathbf{r}_{jk} \cdot \mathbf{F}_e) - \alpha \mathbf{p}_i . \qquad (5)$$

Here, α is the Nosé-Hoover thermostat multiplier acting on the momentum $\mathbf{p}_i$ of atom i. α is calculated using the time integral of the difference between the instantaneous kinetic temperature T of the system and the heat bath temperature T_{eq}, from $\dot{\alpha} = (T - T_{\text{eq}})/Q$, where Q is the thermal inertia. The third term in Eq. (5) guarantees that the net force acting on the entire N-atom system vanishes.

In Fig. 1 we present the results of our nonequilibrium molecular dynamics simulations for the thermal conductance of an isolated (10, 10) nanotube aligned along the z axis. In our calculation, we consider 400 atoms per unit cell, and use periodic boundary conditions. Each molecular dynamics simulation run consists of 50 000 time steps of 5.0×10^{-16} s. Our results for the time dependence of the heat current for the particular value $F_e = 0.2$ Å^{-1}, shown in Fig. 1(a), suggest that $J_z(t)$ converges within the first few picoseconds to its limiting value for $t \to \infty$ in the temperature range below 400 K. The same is true for the quantity $J_z(t)/T$, shown in Fig. 1(b), the average of

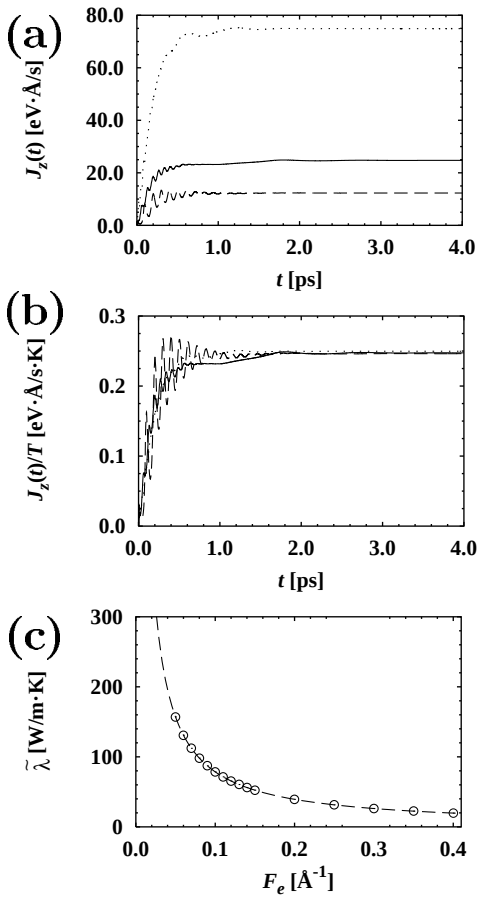

FIG. 1. (a) Time dependence of the axial heat flux $J_z(t)$ in a (10, 10) carbon nanotube. Results of nonequilibrium molecular dynamics simulation at a fixed applied thermal force $F_e = 0.2$ Å^{-1} are shown at temperatures $T = 50$ K (dashed line), 100 K (solid line), and 300 K (dotted line). (b) Time dependence of $J_z(t)/T$, a key quantity for the calculation of the thermal conductivity, for $F_e = 0.2$ Å^{-1} and the same temperature values. (c) Dependence of the heat transport on the applied heat force F_e in the simulations for $T = 100$ K. The dashed line represents an analytical expression that is used to determine the thermal conductivity λ by extrapolating the simulation data points $\tilde{\lambda}$ for $F_e \to 0$.

which is proportional to the thermal conductivity λ according to Eq. (4). Our molecular dynamics simulations have been performed for a total time length of 25 ps to well represent the long-time behavior.

In Fig. 1(c) we show the dependence of the quantity

$$\tilde{\lambda} \equiv \lim_{t\to\infty} \frac{\langle J_z(\mathbf{F}_e, t)\rangle}{F_e T V} \tag{6}$$

on F_e. We have found that direct calculations of $\tilde{\lambda}$ for very small thermal forces carry a substantial error, as they require a division of two very small numbers in Eq. (6). We base our calculations of the thermal conductivity at each temperature on 16 simulation runs, with F_e values ranging from 0.4 to 0.05 Å^{-1}. As shown in Fig. 1(c), data for $\tilde{\lambda}$ can be extrapolated analytically for $\mathbf{F}_e \to 0$ to yield the thermal conductivity λ, shown in Fig. 2.

Our results for the temperature dependence of the thermal conductivity of an isolated (10, 10) carbon nanotube, shown in Fig. 2, reflect the fact that λ is proportional to the heat capacity C and the phonon mean free path l. At low temperatures, l is nearly constant, and the temperature dependence of λ follows that of the specific heat. At high temperatures, where the specific heat is constant, λ decreases as the phonon mean free path becomes smaller due to umklapp processes. Our calculations suggest that at $T = 100$ K, carbon nanotubes show an unusually high thermal conductivity value of 37 000 W/m K. This value lies very close to the highest value observed in any solid, $\lambda = 41\,000$ W/m K, that has been reported [1] for a 99.9% pure ^{12}C crystal at 104 K. In spite of the decrease of λ above 100 K, the room temperature value of 6600 W/m K is still very high, exceeding the reported thermal conductivity value of 3320 W/m K for nearly isotopically pure diamond [16].

We found it useful to compare the thermal conductivity of a (10, 10) nanotube to that of an isolated graphene monolayer as well as bulk graphite. For the graphene monolayer, we unrolled the 400-atom large unit cell of the (10, 10) nanotube into a plane. The periodically repeated unit cell used in the bulk graphite calculation contained 720 atoms, arranged in three layers. The results of our calculations, presented in Fig. 3, suggest that an isolated nanotube shows a very similar thermal transport behavior as a hypothetical isolated graphene monolayer, in general agreement with available experimental data [17–19]. Whereas even larger thermal conductivity should be expected for a monolayer than for a nanotube, we must consider that unlike the nanotube, a graphene monolayer is not self-supporting in vacuum. For all carbon allotropes considered here, we also find that the thermal conductivity decreases with increasing temperature in the range depicted in Fig. 3.

Very interesting is the fact that once graphene layers are stacked in graphite, the interlayer interactions quench the thermal conductivity of this system by nearly 1 order of magnitude. For the latter case of crystalline graphite, we also found our calculated thermal conductivity values to be confirmed by corresponding observations in the basal plane of highest-purity synthetic graphite [17–19] which are also reproduced in the figure. We would like to note that experimental data suggest that the thermal conductivity in the basal plane of graphite peaks near 100 K, similar to our nanotube results.

Based on the above described difference in the conductivity between a graphene monolayer and graphite, we should expect a similar reduction of the thermal conductivity when a nanotube is brought into contact with other systems. This should occur when nanotubes form a bundle or rope, become nested in multiwall nanotubes, or interact with other nanotubes in the "nanotube mat" of "bucky paper" and could be verified experimentally. Consistent with our conjecture is the low value of $\lambda \approx 0.7$ W/m K reported for the bulk nanotube mat at room temperature [4].

In summary, we combined results of equilibrium and nonequilibrium molecular dynamics simulations with

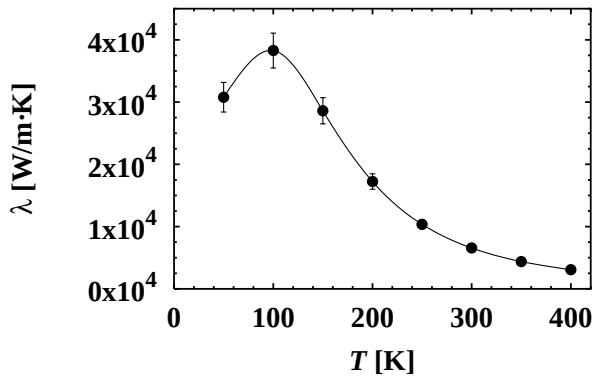

FIG. 2. Temperature dependence of the thermal conductivity λ for a (10, 10) carbon nanotube for temperatures below 400 K.

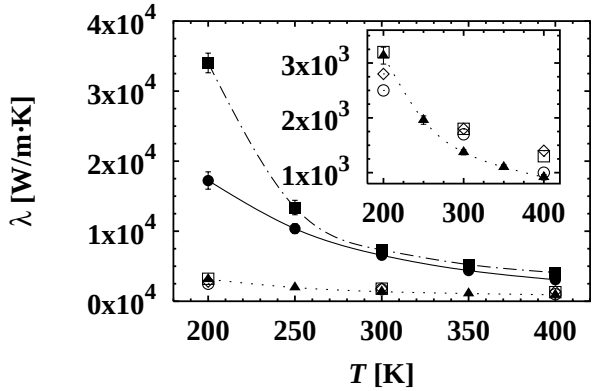

FIG. 3. Thermal conductivity λ for a (10, 10) carbon nanotube (solid line), in comparison to a constrained graphite monolayer (dash-dotted line), and the basal plane of *AA* graphite (dotted line) at temperatures between 200 and 400 K. The inset reproduces the graphite data on an expanded scale. The calculated values (solid triangles) are compared to the experimental data of Refs. [17] (open circles), [18] (open diamonds), and [19] (open squares) for graphite.

accurate carbon potentials to determine the thermal conductivity λ of carbon nanotubes and its dependence on temperature. Our results suggest an unusually high value $\lambda \approx 6600\ \mathrm{W/mK}$ for an isolated $(10, 10)$ nanotube at room temperature, comparable to the thermal conductivity of a hypothetical isolated graphene monolayer or graphite. We believe that these high values of λ are associated with the large phonon mean free paths in these systems. Our numerical data indicate that in the presence of interlayer coupling in graphite and related systems, the thermal conductivity is reduced significantly to fall into the experimentally observed value range.

This work was supported by the Office of Naval Research and DARPA under Grant No. N00014-99-1-0252. We acknowledge useful discussions with Professor Pao-Kuang Kuo and Professor Ctirad Uher.

*Present address: Department of Physics, University of California, and Materials Sciences Division, Lawrence Berkeley Laboratory, Berkeley, CA 94720.

[1] Lanhua Wei, P. K. Kuo, R. L. Thomas, T. R. Anthony, and W. F. Banholzer, Phys. Rev. Lett. **70**, 3764 (1993).
[2] S. Iijima, Nature (London) **354**, 56 (1991).
[3] M. S. Dresselhaus, G. Dresselhaus, and P. C. Eklund, *Science of Fullerenes and Carbon Nanotubes* (Academic Press, San Diego, 1996).
[4] J. Hone, M. Whitney, C. Piskoti, and A. Zettl, Phys. Rev. B **59**, R2514 (1999); J. Hone, M. Whitney, and A. Zettl, Synth. Met. **103**, 2498 (1999).
[5] J. Tersoff, Phys. Rev. B **37**, 6991 (1988).
[6] Citrad Uher, in *Numerical Data and Functional Relationships in Science and Technology*, edited by O. Madelung and G. K. White, Landolt-Börnstein, New Series, Group III, Vol. 15c (Springer-Verlag, Berlin, 1991), pp. 426–448.
[7] Philippe Jund and Rémi Jullien, Phys. Rev. B **59**, 13 707 (1999).
[8] M. Schoen and C. Hoheisel, Mol. Phys. **56**, 653 (1985).
[9] D. Levesque and L. Verlet, Mol. Phys. **61**, 143 (1987).
[10] D. A. McQuarrie, *Statistical Mechanics* (Harper & Row, London, 1976).
[11] A. Maeda and T. Munakata, Phys. Rev. E **52**, 234 (1995).
[12] D. J. Evans, Phys. Lett. **91A**, 457 (1982).
[13] D. P. Hansen and D. J. Evans, Mol. Phys. **81**, 767 (1994).
[14] D. C. Rapaport, *The Art of Molecular Dynamics Simulation* (Cambridge University Press, Cambridge, England, 1998).
[15] S. Nosé, Mol. Phys. **52**, 255 (1984); W. G. Hoover, Phys. Rev. A **31**, 1695 (1985).
[16] T. R. Anthony, W. F. Banholzer, J. F. Fleischer, Lanhua Wei, P. K. Kuo, R. L. Thomas, and R. W. Pryor, Phys. Rev. B **42**, 1104 (1990).
[17] Takeshi Nihira and Tadao Iwata, Jpn. J. Appl. Phys. **14**, 1099 (1975).
[18] M. G. Holland, C. A. Klein, and W. D. Straub, J. Phys. Chem. Solids **27**, 903 (1966).
[19] A. de Combarieu, J. Phys. (Paris) **28**, 951 (1967).